Gate-Tuned High Frequency Response of Carbon Nanotube Josephson Junctions

J.-P. Cleuziou,[1] W. Wernsdorfer,[2] S. Andergassen,[2] S. Florens,[2] V. Bouchiat,[2] Th. Ondarçuhu,[1] and M. Monthioux[1]
[1]*Université de Toulouse, CEMES-CNRS, BP 94347, 31055 Toulouse Cedex 4, France*
[2]*Institut Néel, CNRS/UJF, BP 166, 38042 Grenoble Cedex 9, France*
(Received 8 May 2007; published 11 September 2007)

Carbon nanotube Josephson junctions in the open quantum dot limit are fabricated using Pd/Al bilayer electrodes, and exhibit gate-controlled superconducting switching currents. Shapiro voltage steps can be observed under radio frequency current excitations, with a damping of the phase dynamics that strongly depends on the gate voltage. These measurements are described by a standard resistively and capacitively shunted junction model showing that the switching currents from the superconducting to the normal state are close to the critical current of the junction. The effective dynamical capacitance of the nanotube junction is found to be strongly gate dependent, suggesting a diffusive contact of the nanotube.

DOI: 10.1103/PhysRevLett.99.117001 PACS numbers: 74.50.+r, 73.63.Fg, 73.63.Kv, 74.45.+c

It was recently demonstrated that carbon nanotube (CNT) weak links, connecting two superconducting leads [1], can be gate-controlled Josephson junctions [2–7] and even gate-controlled π junctions [5]. The first interesting application of CNT Josephson junctions are superconducting transistors [3,4] and superconducting quantum interference devices (SQUIDs) [5] being promising candidates for the detection of individual magnetic molecules. They might also prove useful as building blocks for more complicated superconducting devices [8] and new readout schemes [9].

For all theses devices, the critical current I_c and the high frequency response of CNT Josephson junctions play an important role. Indeed, previous investigations showed that the magnitude of the switching current I_{sw} of such CNT devices appeared to be very different from theoretical predictions: in the first experiments it was observed to be 10 times larger [1] and later 10 times smaller [3–7] than the result of Ambegaokar and Baratoff [10], reformulated for a quantum dot (QD) in [11]. Moreover, previous measurements were performed for a static bias, without retrieving the effect of radio frequency (rf) irradiation.

The electronic transport through a CNT junction can be described by a QD in between two conducting leads. The energy level spacing ΔE depends on the length of the junction and the nature of the conducting leads. The transport can be classified into three limits depending on the ratio between the transparency Γ of the QD barriers and the charging energy U [12]. (i) for $h\Gamma \ll U$, the maximum conductance at zero bias obeys $G_{max} \ll 2e^2/h$. In this so-called closed QD regime the charging effects dominate the transport characterized by well-resolved Coulomb blockade diamonds [13]. (ii) for $h\Gamma \approx U$ holds $e^2/h \lesssim G_{max} \lesssim 2e^2/h$. In this intermediate transparency regime charging effects as well as higher-order tunneling processes are very important. Here, transport measurements show that Coulomb blockade diamonds, corresponding to an odd number of electrons, are connected by Kondo ridges [2,14]. For superconducting leads, higher-order multiple Andreev reflections (MARs) are well resolved [2,3]. (iii) For $h\Gamma \gg U$, the conductance is close to $4e^2/h$ and corresponds to the open QD regime, where Coulomb blockade diamonds are not observed. This leads to a relatively high supercurrent for all gate voltages.

An important advantage of these devices is that backgate and sidegate electrodes can be used to vary both Γ and the energy levels position in the nanotube, thus permitting to change the electric transport regime [15]. Similarly, we found that the QD barrier can be varied with the thickness of the Pd contacts, enabling us to access also all three transport regimes. Previous measurements on CNT Josephson junctions were in the intermediated or closed QD regime [16]. Here we present the first measurements in the open QD regime using a Pd thickness of 7 nm. The present description concentrates on a single device, similar data were, however, obtained on a couple of other devices fabricated on the same chip.

The CNT Josephson junction was fabricated as presented earlier [5]. We started from a degenerately n-doped silicon substrate with 350 nm thick thermally grown SiO_2 layer on top used as a backgate. Single-walled CNTs were deposited using a combing technique [17]. The nanotube location was imaged by atomic force microscopy and aligned e-beam lithography patterned the contacts [18]. The length of the tube section between the contacts was about 200 nm. Metal electrodes were deposited using electron-gun evaporation and a thickness of 3 to 7 nm of Pd followed by 50 nm of Al was used. Pd provides high-transparency contacts to the carbon nanotubes. Al is a superconductor having a critical temperature of about 1.2 K. We found that for Pd thicknesses below about 3 nm, the CNT junction was in the closed QD regime, for 4 to 6 nm in the intermediate, and for 7 nm and more in the open QD regime.

The measurements were performed in a shielded cryostat having heavily filtered lines in order to minimize the electronic noise reaching the sample, since electronic noise can reduce and even suppress the switching current of the CNT-SQUID. Our home-built filtering system was presented in [5]. We used mainly a four-probe, current-biased

 © 2007 The American Physical Society

method. High frequency ac current modulations in the frequency range between 1 and 12 GHz was applied with a strongly damped rf line (about -100 dB). The maximal power of the rf source was 10 dBm. The dc and ac lines where connected to the CNT junction via a home-built low-temperature bias tee. Although we control well the relative amplitude of the ac modulation, we do not know the absolute value. However, using the resistively and capacitively shunted junction (RCSJ) model, we can estimate the ac amplitude.

The effective BCS gap Δ_{eff} of the superconducting leads felt by the CNT was estimated by voltage versus current measurements as a function of temperature. We found a transition temperature $T_c = 0.7$ K, yielding a $\Delta_{\mathrm{eff}} = 1.76\, k_B T_c = 0.1$ meV. The energy level spacing of the CNT were determined $\sim$10 meV [5]. However, due to the high transparency of the contacts the effect of the Coulomb energy is much smaller here.

In Figs. 1(a) and 1(b), a magnetic field of $H_z = 50$ mT was applied perpendicular to the electrode plane in order to suppress the superconductivity of the leads. The differential conductivity dI/dV is plotted versus gate voltage at zero bias in Fig. 1(a) and, in addition, as a function of source-drain current I_{sd} in Fig. 1(b). dI/dV oscillates between about 1.8 and 3.5 e^2/h and is I_{sd} independent in the considered range. dI/dV is maximal when a quantum level of the CNT is aligned with respect to the Fermi energy of the leads. A current can then flow by resonant tunneling through the CNT, and we denominate this regime as an on state. When the quantum levels are far from the Fermi energy, the current is reduced (off state). This CNT junction is clearly in the open QD regime because the reduction is only about a factor of 2 and Coulomb blockade effects are not directly observable.

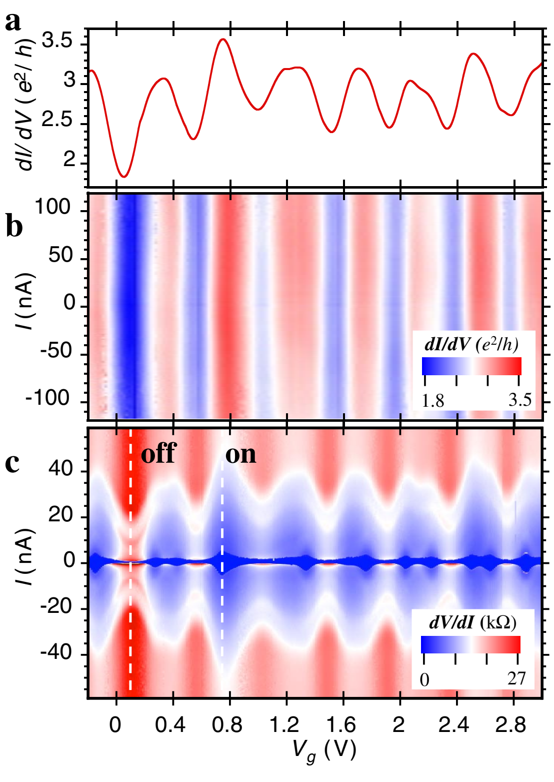

FIG. 1 (color online). Electric transport through a CNT junction as a function of gate voltage V_g. (a) Differential conductivity dI/dV versus V_g at zero bias. (b) dI/dV map versus current bias I_{sd} and V_g in the normal state ($H_z = 50$ mT). (c) Differential resistivity dV/dI map versus I_{sd} and V_g in the superconducting state ($H_z = 0$). The dotted lines indicate the off state and on state, which are further studied in Figs. 2–4.

Figure 1(c) presents the same measurements as in Fig. 1(b) but with superconducting leads ($H_z = 0$). As dI/dV diverges, the differential resistivity dV/dI is plotted. For small I_{sd} a supercurrent is observed, which is evidenced by a nearly zero-resistance state. At a certain bias current denoted by switching current I_{sw}, the junction switches from the superconducting to the normal state. I_{sw} is strongly gate-voltage dependent: it is maximal (minimal) in the on (off) state. Most of the on states are split into two I_{sw} maxima suggesting that there is still a small influence of Coulomb interaction. Note that higher order MARs are not observed, since strong broadening effects can be induced by the high transparency contacts.

Figures 2(a) and 2(b) show typical voltage versus current curves at several temperatures for the on and off state. The on state is characterized by the largest I_{sw} and small hysteresis effects, that is the retrapping current is close to I_{sw}. Furthermore, dV/dI increases for $I_{\mathrm{sd}} > I_{\mathrm{sw}}$ in the considered range. In the off state, the hysteresis effects are very large and dV/dI decreases for $I_{\mathrm{sd}} > I_{\mathrm{sw}}$. A small temperature-dependent resistance is observed at zero bias, which is mainly due to temperature-induced phase diffusion [19].

The high frequency response of the CNT junctions is examined by voltage-current curves in the presence of rf fields. Figures 3(a) and 4(a) show the appearance of constant-voltage Shapiro steps, which are due to the harmonical synchronization of the Josephson oscillations and the applied rf excitations. The steps appear at voltages equal to $nf\phi_0$ where $n = 1, 2, \ldots$ and ϕ_0 is a flux quanta. We checked this linear relation in the frequency range between $f = 1$ to 15 GHz (data not shown). The influence of the rf current I_{rf} on the Shapiro steps is presented on Figs. 3(b) and 4(b) by plots of the differential resistance as a function of I_{rf} and I_{sd}, giving rise to a complicated pattern of nondissipative lobes.

We modeled the data with a phenomenological description of time-dependent transport in superconducting junctions based on both the standard Josephson relations and on classical circuit theory, the so-called RCSJ model [20,21]. This invokes simple differential equations that govern the dynamics of the phase ϕ across the junction:

$$\hbar \frac{d\phi}{dt} = 2\ \mathrm{eV} \tag{1a}$$

$$I(t) = C\frac{dV}{dt} + I_{\mathrm{qp}}(V) + I_c \sin\phi, \tag{1b}$$

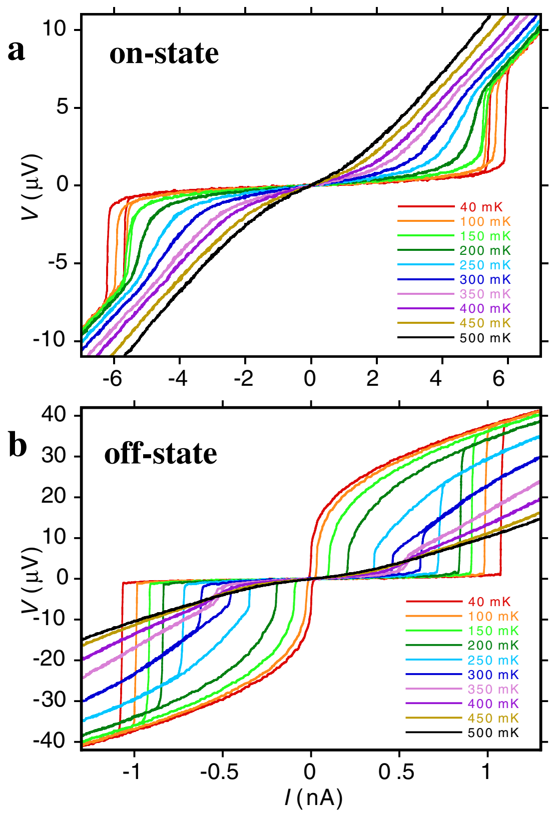

FIG. 2 (color online). Voltage versus current characteristics for a CNT junction in (a) the on state and (b) off state at several temperatures. (a) and (b) correspond to maximal and minimal switching currents in Fig. 1(c), respectively. The current was swept at the sweep rates of 5 and 0.2 nA/s for (a) and (b), respectively. Note that each curve is a single sweep (no data averaging was performed) and the slope at the switching currents was limited by the filtering.

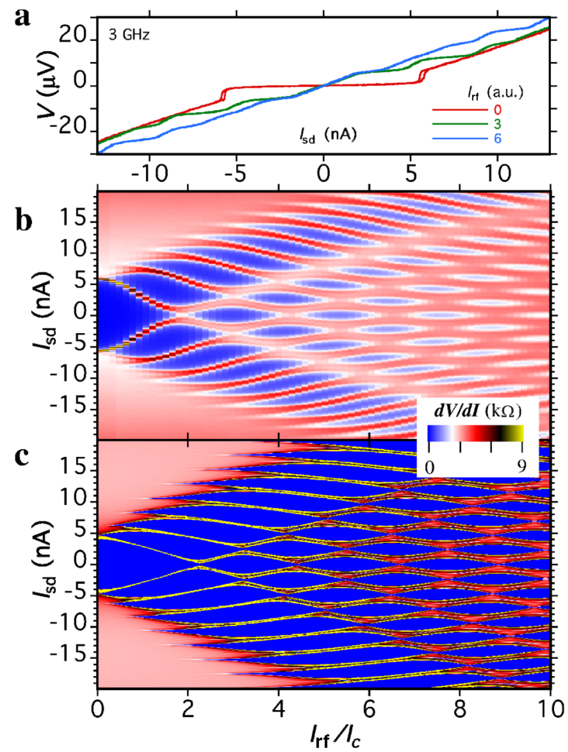

FIG. 3 (color online). rf response in the on state. (a) VI characteristics at several rf amplitudes I_{rf}. (b) Differential resistance dI/dV maps versus I_{sd} and I_{rf} for $f = 3$ GHz. (c) Simulation of the data in (b) using the nonlinear RSJ model.

where V is the instantaneous voltage drop, $I(t) = I_{sd} + I_{rf}\sin(\omega t)$ the injected current with an oscillating part at the radio frequency $f = \omega/2\pi$, $I_{qp}(V)$ the quasiparticle contribution to the current, I_c the critical supercurrent, and C the capacitance of the junction.

Assuming an Ohmic quasiparticle current $I_{qp} = V/R$ and defining a basic frequency scale $\gamma = 2eRI_c/\hbar$, one obtains two relevant dimensionless parameters in the analysis of the Shapiro steps: (i) the reduced pulsation $\tilde{\omega} = \omega/\gamma$ characterizing the shape of the Shapiro steps [22,23] (pure Bessel functions are obtained in the limit $\tilde{\omega} \gg 1$ only); (ii) the quality factor $Q = \sqrt{\gamma RC}$ that controls the damping of the phase dynamics.

The parameters are adjusted to the experimental data in the rf driven regime where the dynamics is less sensitive to phase diffusion [19]. The analysis of the experimental data in the on state reveals a globally good agreement for $Q \lesssim 1$, i.e., the RSJ model with no capacitance. Indeed, the geometrical capacitance of CNT junctions is very small (~ 30 aF). This finding is supported by the small hysteresis effects of the VI curves [Fig. 2(a)]. Note that the predicted I_c is very close to I_{sw} at $I_{rf} = 0$. The Shapiro step positions present, however, small but appreciable deviations to the pure Bessel functions. Their precise shape can indeed be more accurately described using a reduced pulsation $\tilde{\omega} \sim 0.35$. Furthermore, a clear downward dispersion of the lobes is observed, which may be attributed to the non-Ohmic character of the quasiparticle current $I_{qp}(V)$ above the threshold I_{sw}. Simulations of the phase dynamics with such nonlinear RSJ model, where the nonlinear R from the VI curves in the resistive state of Fig. 2 was included, are provided in Fig. 3(c) and compare favorably to the experimental data (for further detail, see [24]).

Regarding the off state, several issues point to additional underdamping effects: the VI curves are strongly hysteretic and the degree of hysteresis diminishes with increasing temperature [Fig. 2(b)] [21]. Moreover, the low-bias Shapiro steps present a peculiar threshold behavior [Fig. 4(b)], while the lobes show an upward dispersion. These properties cannot be explained within the usual RCSJ model, and may be only accounted for at a qualitative level by introducing a rather large effective capacitance $C \approx 1$ fF and a nonlinear quasiparticle resistance (stronger than in the on state discussed above). Figure 4(c) shows a partial agreement between our simulations and the data. The gate dependence of C suggests a diffusive CNT contact in the off state, i.e., additional capacities coming from the CNT contacts. Indeed, for the off state, the electrode or nanotube capacitance has to be taken into account since the Pd or nanotube contact is

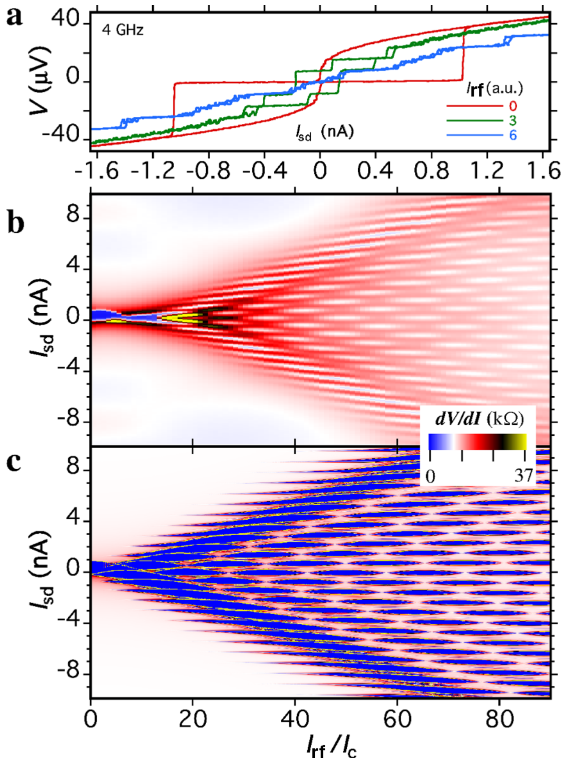

FIG. 4 (color online). rf response in the off state. (a) VI characteristics at several $I_{\rm rf}$. (b) dI/dV maps versus $I_{\rm sd}$ and $I_{\rm rf}$ for $f = 4$ GHz. (c) Simulation of the data in (b) using the nonlinear RCSJ model.

known to be distributed over a larger part of the contact [25]. Its value can be rather large (~ 1 fF). For the on state, however, the capacitance of the contact can be strongly renormalized by the tunnel effect [26] and the capacitance of the junction is mainly due to the nanotube self-capacitance estimated as 30 aF for a nanotube portion of 200 nm [27]. A more thorough analysis of quantum and thermal fluctuation effects on the Shapiro steps in the spirit of Refs. [28,29] is clearly beyond the scope of the present study. We point out, however, that these effects probably do not account for the strong reduction of the critical current, as the above analysis demonstrated in the on state.

In conclusion, we studied the critical currents and the constant-voltage Shapiro steps under rf irradiation of a strongly coupled CNT Josephson junction, and discovered a strong gate-voltage dependence. These junctions are therefore very promising as tunable rf building blocks for superconducting devices.

This work was partially supported by the CNRS ACI NOCIEL and ANR QuSpins. Clean room processes were supported by the CNRS RTB program in the technological facilities of the LAAS (Laboratory for Analysis and Architecture of Systems, University of Toulouse, France). We thank F. Balestro, O. Buisson, F. Carcenac, J. Clarke, E. Eyraud, D. Feinberg, and I. Siddiqi for important contributions and helpful discussions.

[1] A. Y. Kasumov *et al.*, Science **397**, 598 (1999).
[2] M. R. Buitelaar, T. Nussbaumer, and C. Schonenberger, Phys. Rev. Lett. **89**, 256801 (2002); **91**, 057005 (2003).
[3] P. Jarillo-Herrero, J. A. van Dam, and L. P. Kouwenhoven, Nature (London) **439**, 953 (2006).
[4] H. I. Jorgensen, K. Grove-Rasmussen, T. Novotny, K. Flensberg, and P. E. Lindelof, Phys. Rev. Lett. **96**, 207003 (2006).
[5] J.-P. Cleuziou, W. Wernsdorfer, V. Bouchiat, Th. Ondarçuhu, and M. Monthioux, Nature Nanotechnology **1**, 53 (2006).
[6] T. Tsuneta, L. Lechner, and P. J. Hakonen, Phys. Rev. Lett. **98**, 087002 (2007).
[7] A. Eichler *et al.*, arXiv:cond-mat/0703082 [Phys. Rev. Lett. (to be published)].
[8] I. Chiorescu, Y. Nakamura, C. J. P. M. Harmans, and J. E. Mooij, Science **299**, 1869 (2003).
[9] I. Siddiqi *et al.*, Phys. Rev. Lett. **93**, 207002 (2004); **94**, 027005 (2005).
[10] V. Ambegaokar and A. Baratoff, Phys. Rev. Lett. **10**, 486 (1963).
[11] C. W. J. Beenakker and H. van Houten, arXiv:condmat/0111505.
[12] For short CNT junction of few 100 nm, $\Delta E > h\Gamma$, U.
[13] D. H. Cobden and J. Nygard, Phys. Rev. Lett. **89**, 046803 (2002).
[14] D. Goldhaber-Gordon *et al.*, Phys. Rev. Lett. **81**, 5225 (1998).
[15] J.-P. Cleuziou, W. Wernsdorfer, V. Bouchiat, Th. Ondarçuhu, and M. Monthioux, arXiv:cond-mat/0610622.
[16] The data in [3] were interpreted to be in the open QD regime. However, the well-resolved higher-order MAR fine structures as well as the high resistivity in the off state may suggest that these devices operated in the intermediate transport regime.
[17] S. Gerdes, T. Ondarçuhu, S. Cholet, and C. Joachim, Europhys. Lett. **48**, 292 (1999).
[18] M. Sagnes *et al.*, Microelectron. Eng. **67**, 683 (2003).
[19] D. Vion, M. Gotz, P. Joyez, D. Esteve, and M. H. Devoret, Phys. Rev. Lett. **77**, 3435 (1996).
[20] A. Barone and G. Paterno, *Physics and Applications of the Josephson Effect* (John Wiley and Sons, New York, 1982), Vol. 1.
[21] M. Tinkham, *Introduction to Superconductivity* (McGraw-Hill, New York, 1996), 2nd ed., Vol. 1.
[22] K. K. Likharev and V. K. Semenov, Radiotech. Elektron. **16**, 2167 (1971).
[23] P. Russer, J. Appl. Phys. **43**, 2008 (1972).
[24] S. Andergassen and S. Florens (to be published).
[25] N. Nemec, D. Tomanek, and G. Cuniberti, Phys. Rev. Lett. **96**, 076802 (2006).
[26] K. Flensberg, Phys. Rev. B **48**, 11 156 (1993).
[27] Note that in the on state we neglected the quantum capacitance of the nanotube, which is estimated ~100 aF. See also S. Rosenblatt *et al.*, Nano Lett. **2**, 869 (2002); S. Ilani, L. A. K. Donev, M. Kindermann, and P. L. McEuen, Nature Phys. **2**, 687 (2006).
[28] Y. M. Ivanchenko and L. A. Zilberman, Sov. Phys. JETP **28**, 1272 (1969).
[29] R. Duprat and A. Levy Yeyati, Phys. Rev. B **71**, 054510 (2005).